

Imaging Biomarkers of Contrast-enhanced Computed Tomography Predict Survival in Oesophageal Cancer After Definitive Concurrent Chemoradiotherapy

Chengbing Zeng

Shantou University Medical College Cancer Hospital

Tiantian Zhai

Shantou University Medical College Cancer Hospital

Jianzhou Chen

University of Oxford

Longjia Guo

Shantou University Medical College Cancer Hospital

Baotian Huang

Shantou University Medical College Cancer Hospital

Hong Guo

Shantou University Medical College Cancer Hospital

Guozhi Liu

Shantou University Medical College Cancer Hospital

Tingting Zhuang

Shantou University Medical College Cancer Hospital

Weitong Liu

Shantou University Medical College Cancer Hospital

Ting Luo

Shantou University Medical College Cancer Hospital

Yanxuan Wu

Shantou University Medical College Cancer Hospital

Guopeng Peng

Shantou University Medical College Cancer Hospital

Derui Li

Shantou University Medical College Cancer Hospital

Chuangzhen Chen (✉ stccz@139.com)

Shantou University Medical College Cancer Hospital <https://orcid.org/0000-0002-2342-8099>

Research

Keywords: esophageal cancer, image biomarker, computed tomography, Prognosis

Posted Date: June 11th, 2020

DOI: <https://doi.org/10.21203/rs.3.rs-33598/v1>

License:   This work is licensed under a Creative Commons Attribution 4.0 International License.

[Read Full License](#)

Version of Record: A version of this preprint was published on January 12th, 2021. See the published version at <https://doi.org/10.1186/s13014-020-01699-w>.

Abstract

Background: This study aimed to evaluate the predictive potential of contrast-enhanced computed tomography (CT)-based imaging biomarkers (IBMs) for the treatment outcomes of oesophageal squamous cell carcinoma (OSCC) patients after definitive concurrent chemoradiotherapy (CCRT).

Methods: A total of 151 ESCC patients who underwent definitive CCRT were included in this retrospective study. All patients were separated randomly to a training cohort (n=97) and the validation cohort (n=54). Pre-treatment contrast-enhanced CT scans were obtained for all patients and used for the extraction of IBMs. An IBM score was constructed by using the least absolute shrinkage and selection operator with logistic regression analysis in training cohort and tested in the validation cohort. IBMsnomograms were built based on IBM score. The concordance index (C-index) was used to assess the performance of the nomograms. Finally, decision curve analysis was performed to estimate the clinical usefulness of the nomograms.

Results: A total of 96 IBMs were extracted from each contrast-enhanced CT scan. The IBM score were consisted of 13 CT-based IBMs and were significantly correlated with 3-year overall survival (OS) and 3-year progression-free survival (PFS). Multivariate analysis revealed that IBM score was the independent prognostic factor. In the training cohort, the IBM score yielded an area under the curves (AUCs) of 0.802 (95% CI: 0.713–0.891, $p < 0.001$) and 0.742 (95% CI: 0.620–0.889, $p < 0.001$) in terms of 3-year OS and 3-year PFS, respectively. In validation cohort, the AUCs were 0.761(95% CI: 0.639–0.900, $p < 0.001$) and 0.761(95% CI: 0.629–0.893, $p = 0.001$) for 3-year OS and 3-year PFS, respectively. Kaplan-Meier survival analysis showed significantly different between risk subgroups in training and validation cohort. The nomograms were built based on the IBM score showed good discrimination. In the training cohort, with the C-indices of IBMsnomograms were 0.732 (95%CI, 0.661–0.803) and 0.670(95%CI, 0.595–0.745) for OS and PFS, respectively. In the validation cohort C-indices were 0.677(95%CI, 0.583–0.771) and 0.678(95%CI, 0.591–0.765) for OS and PFS, respectively. The decision curve showed the clinical usefulness of nomograms.

Conclusions: TheIBM score based on pre-treatment contrast-enhanced CT could predict the 3-year OS and 3-year PFS for OSCC patients after definitive CCRT. Further multicenter studies with larger sample sizes are warranted.

Background

Esophageal cancer (EC) is one of the most common cancers globally, and in 2018, its incidence and number of cancer-related deaths ranked the seventh and sixth, respectively [1]. The management of EC typically involves multidisciplinary therapy, including definitive concurrent chemoradiotherapy (CCRT), which is the main standard treatment for esophageal squamous cell carcinoma (ESCC) for medically unresectable tumors and is also an option for resectable tumors. However, the outcomes of CCRT among these patients are still disappointing, with 3-year overall survival (OS) rates of 23–44.7% [2–5]. More than

50% of patients in the RTOG 85 – 01 trial and INT 0123 trial locoregional experienced disease progression [3, 5]. Patients with higher mortality risk after CCRT may benefit from more intensive primary treatment (e.g. planned radical surgery after CCRT), adjuvant therapy (e.g. chemotherapy), or more frequent follow-up. The application of these strategies requires the identification of patients with high mortality risk prospectively to achieve personalized management. Thus, to improve the overall survival of EC patients after CCRT, it is crucial to predict the mortality risk of each individual patient.

Prediction of outcomes among EC patients after CCRT remains an unmet clinical need. One of the most commonly used methodologies for prognostic evaluation in the clinic is the TNM staging system, which stratifies patients into different stages according to their tumor burden. Although the clinical staging system could provide important insights for evaluating outcomes of patients with different stages, its role in survival prediction among patients with the same disease stage is insignificant. Indeed, previous studies have shown that the clinical staging system fails to predict heterogeneous outcomes of patients with locally advanced disease after CCRT [6–8]. A variety of other clinical factors and biomarkers have also been assessed for their prognostic potential [9–11]. Yet, none of these factors have been widely used for the clinical stratification of patients and decision-making, as each of them has weaknesses and limitations.

Besides clinical factors and biomarkers, quantitative imaging biomarkers (IBMs) might become an interesting source in multiple cancer types by using imaging techniques currently. These so-called radiomics could extract a great amount of information from commonly available images with a high throughput [12–14]. Previous studies have reported the potential prognostic information of computed tomography (CT) textural features in EC, and were able to assess and predict histopathological characteristics, treatment response, or survival outcome among EC patients to some extent [15–19]. The CT scans play an important role in the radiation treatment of EC, including diagnosis, staging, treatment planning, quality control, and follow-up. Plain CT-based IBMs have been shown to be correlated with patients' outcomes in a number of cancer types, including ESCC [18, 20]. However, the most commonly available imaging modality for patients after undergoing definitive CCRT were not plain CT scans but contrast-enhanced CT scans which were performed during treatment planning. A previous study suggested that post-treatment IBMs extracted from contrast-enhanced CT images might have a correlation with OS in EC patients who received definitive CCRT [16]. Although the sample size of this study was small and only included 26 cases of squamous cell carcinoma (SCC), it was instructive for further studies. The commonest pathological type of EC in China is SCC, and radiotherapy is administered with a total dose of 60–66 Gy [21]. This range was much higher than the dose used in the standard treatment of EC via conventional fractionated radiotherapy (50.4 Gy). Esophageal edema is a common acute adverse event after definitive CCRT. There are fewer residual lesions that could be used for objective analysis or evaluation after definitive CCRT. Further, some patients with complete response did not have residual lesions. It is unclear whether contrast-enhanced CT images obtained before treatment could serve as a feasible source for radiomics analysis in ESCC. Therefore, stronger evidence was needed in support of the implications for survival outcomes and the reliability of the methodology.

In this study, we sought to develop and validate an IBM score to predict 3-year OS and 3-year progression-free survival (PFS) for ESCC patients and assessed its value for individual OS and PFS estimation.

Methods

Patients

The protocol for this retrospective study was obtained from the local ethics and institutional review board. Approval and the need for informed consent has been waived. This study included patients with EC who underwent definitive CCRT at AAA between September 2009 and August 2015. The inclusion criteria were: (1) pathological diagnosis of ESCC; (2) primary tumor located in the cervical, upper thoracic, or middle thoracic esophagus; and (3) contrast-enhanced CT scan findings, which were used in treatment planning before definitive CCRT. The exclusion criteria were: (1) patients who only received radiotherapy or chemotherapy; (2) prior surgery or administration of chest radiotherapy or chemotherapy; and (3) a follow-up time < 36 months or unknown survival status. As shown in Fig. 1, the final study population consisted of 151 patients. All patients received intensity modulated radiation therapy (IMRT) combined with chemotherapy. Of these, 78 ESCC patients were from a phase II prospective clinical study, using simultaneous modulated accelerated radiotherapy (SMART) combined with chemotherapy [22]. One hundred and fifty-one patients were randomly assigned into a training cohort (n = 97) and validation cohort (n = 54).

All patients underwent simulated CT scans for treatment planning. Seventy-eight patients had undergone SMART, followed by radiation therapy with a prescribed dose of 66 Gy/30F, 5 days per week. Other patients underwent radiation therapy with a prescribed dose of 64/32F, 5 days per week. Most patients (91.4%) received concurrent chemotherapy based on the cisplatin and 5-fluorouracil (PF) regimen. The intensity of concurrent chemotherapy was relatively reduced among patients with advanced age or poor performance status. Data regarding clinical characteristics of patients were collected in both cohorts, including age, gender, clinical stage, and tumor location. Dose-volume information for the primary tumor was collected from the radiotherapy planning system. Further details are shown in Table 1.

Table 1
Clinical characteristics of 151 patients with ESCC after definitive CCRT

Factors	Training cohort n (%)	Validation cohort n (%)	p-value
Age, years			0.094 ^b
Median (range)	61 (37–76)	58 (40–76)	
Gender			0.732 ^c
Male	76 (78.4%)	41 (75.9%)	
Female	21 (21.6%)	13 (24.1%)	
Tumor location			0.388 ^c
Cervical	16 (16.5%)	12 (22.2%)	
Upper	52 (53.6%)	31 (57.4%)	
Middle	29 (29.9%)	11 (20.4%)	
T stage ^a			0.444 ^c
T2	11 (11.3%)	10 (18.5%)	
T3	44 (45.4%)	24 (44.4%)	
T4	42 (43.3%)	20 (37.3%)	
N stage ^a			0.571 ^c
N0	35 (36.1%)	22 (40.7%)	
N1	62 (63.9%)	32 (59.3%)	
M stage ^a			0.671 ^c
M0	85 (87.6%)	46 (83.2%)	
M1	12 (12.4%)	8 (14.8%)	

Abbreviations: ESCC, esophageal squamous cell carcinoma; CCRT, concurrent chemoradiotherapy; AJCC, American Joint Committee on Cancer (AJCC) staging system (version 6.0); RT, radiotherapy; PF, cisplatin and 5-fluorouracil.

^a According to American Joint Committee on Cancer (AJCC) staging system 6th

^b p-value was analyzed using the independent samples *t*-test

^c p-value was analyzed using the chi-squared test

Factors	Training cohort n (%)	Validation cohort n (%)	p-value
Clinical stage ^a			0.893 ^c
Ⅹ stage	28 (28.9%)	16 (29.4%)	
Ⅹ stage	57 (58.8%)	30 (55.6%)	
Ⅹ stage	12 (12.4%)	8 (14.8%)	
Chemotherapy regimen			0.413 ^c
RT with PF	90 (92.8%)	48 (88.9%)	
RT with other regimens	7 (7.2%)	6 (11.1%)	
Dose regimen			0.096 ^c
2.2 Gy × 30 F	55 (56.7%)	23 (42.6%)	
2.0 Gy × 32 F	42 (43.3%)	31 (57.4%)	
Abbreviations: ESCC, esophageal squamous cell carcinoma; CCRT, concurrent chemoradiotherapy; AJCC, American Joint Committee on Cancer (AJCC) staging system (version 6.0); RT, radiotherapy; PF, cisplatin and 5-fluorouracil.			
^a According to American Joint Committee on Cancer (AJCC) staging system 6th			
^b p-value was analyzed using the independent samples <i>t</i> -test			
^c p-value was analyzed using the chi-squared test			

Contrast-enhanced Ct Image Acquisition

The CT scans of all patients were acquired (Philips Brilliance CT Big Bore Oncology Configuration, Cleveland, OH, USA; voxel size: $1.0 \times 1.0 \times 3.0 \text{ mm}^3$ for 79 patients and $1.0 \times 1.0 \times 5.0 \text{ mm}^3$ for 72 patients; convolution kernel: Philips Healthcare's B), using a scanning voltage of 120 kVp with a slice thickness of 3–5 mm after an intravenous injection of 75 ml of 300 mg/mL iodinated contrast agent at a rate of 1.8–2 mL/sec with a pump injector (Medrad Stellant; Bayer, Beijing, China). The CT images were transmitted to the radiation therapy planning system (Eclipse Planning System version 10.0) via the DICOM 3.0 port.

Region Of Interest (roi) Delineation And Ibms Extracted

Pre-treatment contrast-enhanced CT scan images of patients were exported for analysis. The primary tumor was delineated by experienced radiation oncologists on the mediastinal window of the planning CT scan. IBMs were extracted by internal programming software using MATLAB R2016a (Mathworks,

Natick, USA) and its toolbox. From the contrast-enhanced CT images of each patient, 96 IBMs were extracted, including the following types: (1) 24 CT intensity IBMs, describing the distribution of voxel parameter values in the volume of interest, such as the min, max and skewness of the primary tumor intensity. (2) Overall, 20 geometric IBMs, calculating the size and shape of the volume of interest, such as sphericity, volume, surface and long axis length. (3) Overall, 52 texture IBMs, describing the difference in voxel density distribution of the three-dimensional contoured structure, consisted of four different matrices: gray level co-occurrence (GLCM) [23], gray level run-length (GLRLM) [24], neighborhood gray-tone difference (NGTDM) [25], and gray level size-zone (GLSZM) matrices [26]. More details on the algorithms for IBM extraction and application have been discussed in previous studies [14, 27].

Outcome Ibm Score And Nomogram Construction

The measured outcome was modeled as a function of clinical and biological variables. We performed the least absolute shrinkage and selection operator (LASSO) for the logistic algorithm to select IBMs that were highly associated with 3-year OS or 3-year PFS. LASSO was not only suitable for regression analysis of high-dimensionality data, but also allowed for the avoidance of model over-fitting because of collinearity of the covariates. In order to eliminate the extent of redundancy between features and considering the prognostic ability of them, all 96 IBMs were incorporated into the analysis. LASSO methods assessed the worth of a subset of preferred low inter-correlation features that are highly associated with outcomes [28]. The LASSO algorithm with 10-fold cross-validation was used to select the final IBMs by determining the optimal value of λ . The formula were developed based on the selected IBMs and their corresponding LASSO coefficients, then used to calculate a multiple-IBM-based score (defined as the IBM score) for each patient to reflect the risk of mortality or tumor progression. Multivariable logistic proportional hazards analysis was used to assess the IBM score as an independent predictor by integrating clinical risk factors. And variance inflation factor (VIF) used to evaluate the collinearity among these final IBMs. In the training cohort, the nomograms based on the IBM score were developed to assess individual patient-level probability estimates for 1-year, 2-year, and 3-year OS or PFS rates according to each patient's unique combination of baseline characteristics.

Prognostic Performance Evaluation

As ESCC patients were assigned into two cohorts, the performance of the IBM score were evaluated by receiver operating characteristic (ROC) curve analysis. ROC curves were plotted for both the training and validation cohorts. The optimal cut-off values of the ROC curves were determined using the Youden Index (YI) in the training cohort. Accordingly, patients were stratified by the maximum YI in two cohorts. Kaplan-Meier survival curve analyses were used to compare differences in OS between high and low risk subgroups using log-rank tests. Further, the concordance index (C-index) was used to quantify the discrimination power of the nomograms. To compared with the utility of clinical stage, decision curve

analysis (DCA) was used to evaluate the net benefits between IBMs nomograms and clinical stage at different threshold probabilities in both cohorts.

Follow-up

The survival estimates mainly assessed in this study were 3-year OS and 3-year PFS. 3-year OS was defined as recording survival status with 3 years of follow-up time as the cut-off point. 3-year PFS defined as recording of the first relapse at any site or death due to any cause with 3 years of follow-up time as the cut-off point. The second secondary end point was OS and PFS, OS was defined as the time from the beginning of radiation therapy to death due to any cause or the last day of clinical follow-up. PFS was defined as the time from the beginning of radiation therapy to first relapse at any site or death from any cause, whichever occurred first, or the last day of clinical follow-up.

Statistical analysis

The clinical features of the patients in the two cohorts were compared using the independent *t*-test or chi-squared test, for a statistical significance level of 0.05 for a two-sided test. All statistical analyses were performed using R version 3.6.0 (The R Foundation for Statistical Computing, Vienna, Austria) and SPSS version 23.0 (IBM Corp, Armonk, NY, USA). The LASSO algorithm was implemented using the *glmnet* package in the R environment [29]. The ROC curves were plotted using the *pROC* package and Kaplan-Meier curves were using the *survminer* package in the R environment. Nomograms were constructed using the *rms* and *survival* packages in the R environment. The DCA curves were using the *rmda* package in the R environment.

Results

Baseline clinical results

The clinical factors for the training and validation cohorts were listed in Table 1. No significant differences in patient clinical characteristics were found between the two cohorts. Of the 151 patients included in the study, 117(77.5%) were men, and the median (inter-quartile range, IQR) age of all patients was 60(55–65). In the training cohort, the median (IQR) survival time for OS and PFS were 44(19–59.5) and 37(10–56.5) months, respectively. In the validation cohort, the median (IQR) survival time for OS and PFS were 37.5 (21.75–55) and 36 (11.75–54.25) months, respectively.

Feature Extraction Results

A LASSO Logistic regression model was used to build the prognostic models, which selected 13 potential predictors from the 96 IBMs in the training cohort. We plotted the binomial deviance versus $\log(\lambda)$, where λ is the tuning parameter (Figure S1). A dotted vertical line was drawn at $\log(\lambda) = -2.88923$, which

corresponded to the best value $\lambda = 0.05561901$. The optimal tuning parameter resulted in 13 non-zero coefficients. With their corresponding coefficients in the LASSO Logistic regression analysis, the calculation formula of IBM score was constructed (Supplementary Materials). Regarding the collinearity diagnosis, the VIFs of the thirteen IBMs were acceptable, range from 1.100–8.151, indicating that there is no collinearity problem.

Assessment Of The Performance Of Ibm Score

We assessed the prognostic accuracy of the IBM score in training cohort using 3-year ROC analysis (Fig. 2A). The area under the curves (AUCs) of the IBM score were 0.802 (95% CI: 0.713–0.891, $p < 0.001$) and 0.742 (95% CI: 0.620–0.889, $p < 0.001$) in terms of 3-year OS and 3-year PFS. Then, we performed the same analysis in validation cohort and similar results were observed (AUCs were 0.761(95% CI: 0.639–0.900, $p < 0.001$) and 0.761(95% CI: 0.629–0.893, $p = 0.001$), respectively; Fig. 2B).

According to the maximum YI, the optimal cut-off value generated by ROC curve was -0.7213013625 . Accordingly, the patients were stratified into a high-risk subgroup (IBM score ≥ -0.7213013625), and a low-risk subgroup (IBM score < -0.7213013625). In the training cohort, the 3-year OS and 3-year PFS were 92.7% and 73.2%, respectively, for the low-risk subgroup; 42.9% and 33.9%, respectively, for the high-risk subgroup (hazard ratios [HRs] 4.920 (95%CI, 2.258–10.719) and 2.796(95%CI, 1.498–5.218), respectively; all $P < 0.001$, log-rank test; Fig. 3A). Similar results were observed in the validation cohort, the 3-year OS and PFS were 78.9% and 73.7%, respectively, for the low-risk subgroup; 42.9% and 40.0%, respectively, for the high-risk subgroup (HR 2.957 (95%CI, 1.104–7.919) and 2.610 (95%CI, 1.050–6.488), respectively; all $P < 0.05$; Fig. 3B).

ESCC patient with higher IBM score were more likely to have death and tumor-progression. In univariable logistic regression analysis, high IBM score patients were correlated with significantly poorer 3-year OS and PFS (Table S1). Factors demonstration a significant effect on 3-year OS and 3-year PFS were included in the multivariable analysis. Multivariable logistic regression analysis for clinical factors revealed that the IBM score remained a powerful and independent prognostic factor for 3-year OS and 3-year PFS in the training and validation cohorts (Table S2 and S3). And no clinical factor was identified as independent prognostic factor in the multivariable logistic regression analysis.

Assessment Of Ibms Nomograms In Os And Pfs Performance

The IBMs nomograms, incorporating IBM score for OS and PFS, were constructed (Fig. 4). In the training cohort, the C-indices of OS and PFS nomogram were 0.732 (95%CI, 0.661–0.803) and 0.670(95%CI, 0.595–0.745), respectively. Similar results were observed in the validation cohort, the C-indices were 0.677(95%CI, 0.583–0.771) and 0.678(95%CI, 0.591–0.765), respectively. The value of C-index showed that the IBMs nomograms had a good prognostic effect in the training and validation cohorts. The

decision curve analysis presented that IBMs nomograms had higher overall net benefit than the clinical stage, within a major range of reasonable threshold probability (Fig. 5). Compared to the clinical stage, the IBMs nomograms showed better discrimination capability in the training and validation cohorts.

Discussion

This study showed that IBMs from contrast-enhanced CT images might yield to predict 3-year OS and 3-year PFS for EC patients. An IBM score was revealed to be an independent prognosis factor for ESCC patients. Patients were successfully stratified into low-risk and high-risk subgroups by the IBM score, with significant differences in OS and PFS. The IBMs nomograms showed better discrimination capability than the traditional clinical staging, indicating the clinical value of the IBM score for individualized OS and PFS estimation to some extent.

The newly IBM score, consisting of 13 optimal IBMs, demonstrated to be significant associated with ESCC patients for 3-year OS and 3-year PFS. Range, Q75, Q975 were obtained from the histogram of voxel intensities and represented the heterogeneity of voxel intensities within the ROI [27]. The geometric IBMs, Sphericity and Major Axis Length, quantified the spherical and size nature of tumor. These IBMs can promote the objective evaluation of subtle changes within tumors and provide clues on lesion invasiveness and growth-patterns [30, 31]. A higher value of texture IBMs, included Maximum Probability, Sum of Square Variance and Low Gray Level Run Emphasis, indicated the greater distribution variability of gray-level intensity values in the image [32, 33]. Small Zone Emphasis measures the distribution of small size zones and small dependencies, and Zone Percentage assessed the distribution of large zones of the same intensity, and not of small groups of pixels or segments in any given direction [26, 34]. These texture IBMs containing spatial information among voxels could strongly reflect intra-tumor heterogeneity which was highly relevant to poor prognosis [12]. In order to correlate the multiple IBMs with pathophysiological basis of tumor in an intuitive method, we constructed the multi-feature IBM score, which provided novel oncological biomarkers for obtaining phenotypic information, potentially assisting clinicians in making management strategies.

Current guidelines recommended definitive CCRT as a standard component for locally advanced ESCC therapies. However, some studies suggested that subgroups of patients could not show to be beneficial from present definitive CCRT strategies. Therefore, accurately distinguishing the risk subgroups of ESCC patients will help improve the current prognostic system and guide more personalized treatment. A few studies have focused on the correlate between radiomics analysis and treatment outcomes evaluation. Zhai et al. [30] found that heterogeneous IBMs on CT images were significantly correlated with OS and helped improve the performance of clinical factors for OS among head and neck cancer patients. Mule et al. [35] investigated contrast-enhanced CT outcomes that might help predict survival in patients with advanced hepatocellular carcinoma treated with sorafenib. In the present study, we indicated that ESCC patients with higher IBM scores had a greater likelihood of worse survival rate and failed to response to CCRT. High-risk ESCC patients identified in the present studies might lead to an appropriate group for more effective systemic approaches to improve survival outcomes [36, 37]. Thus, the IBM score was a

prognostic tool for ESCC patients after definitive CCRT. Therefore, patients with higher IBM score would have larger probability of poor survival outcomes.

TNM staging system is the most useful tool to stratify ESCC patients into different stages according to their tumor burden. However, its role in survival prediction among ESCC patients with the same clinical stage were insignificant. To develop an individualized easy-to-use tool for clinicians, we attempted to construct nomograms based on IBM score for the prediction of the prognosis of individual patients. These IBMs nomograms could be used to predict the probability of 1-year, 2-year and 3-year OS and PFS for individual ESCC patient. The nomograms performed well with significant C-index and showed good discrimination and clinical utility both in the training and validation cohorts, such as helping counsel patients, individualize therapy, and arrange the follow-up for ESCC patients. The decision curve analysis indicated that the IBM score was superior to the clinical stage, within a major range of reasonable threshold probability. Notably, the limited performance and validation of the IBM score was that it was developed based on 3-year OS and 3-year-PFS, and it might result in the lack of some prognostic information. Encouragingly, the IBMs nomograms still had good predictive power for OS and PFS. One possible explanation was that most deaths or tumor progression in ESCC patients after definitive CCRT would occur within 3 years follow-up [2, 3]. In our study, during the follow-up time, 3-year OS rate and 3-year PFS rates were 60.9% and 51.0%, respectively, while OS and PFS rates were 55.6% and 48.3%, respectively. However, more appropriate approaches for assessment of prognosis model for ESCC patients was needed to establish in the future.

For EC patients, contrast-enhanced CT scan is the main performed imaging tool in conventional clinical practice [38]. It has been reported that IBMs extracted from contrast-enhanced CT images might be correlated with the spatial variability in microvessel density [39]. However, in standard CT images, IBMs might be associated with the variability in tissue densities due to spatially variable fibrosis, cell density, and necrosis [13]. Badic et al. suggested that IBMs extracted from standard CT and contrast-enhanced CT images could provide complementary prognostic information from both approaches [40]. In view of the wide availability of contrast-enhanced CT scans among patients undergoing definitive radiotherapy, our study provides an important basis for conducting large-scale and multicenter research. It is important to note that quality assurance of contrast-enhanced CT scans will have a critical impact on radiomics based on these images. Furthermore, verification is needed on whether IBMs extracted from contrast-enhanced CT images could provide prognostic information for esophageal adenocarcinoma patients.

The limitations of our retrospective design include several aspects that were insufficient for the model [41]. This was a retrospective and single-center study, including the relatively small sample size. This would be addressed more thoroughly in the future by using a greater sample size with multicenter validation cohorts to acquire high-level evidence for survival outcomes. Compared to IBM score, the clinical factors showed poor discrimination ability in predicting 3-year OS and 3-year PFS used in this study, but other potential prognostic biomarker should be incorporated into our IBMs nomograms. A combination of multiple biomarkers and IBMs may improve the capability of predicting 3-year OS among ESCC patients underwent definitive CCRT.

Conclusions

We demonstrated that the IBMs extracted from contrast-enhanced CT images showed good predictive performance for su among ESCC patients. Moreover, IBM score might be a non-invasive predictive tool to guide individualized treatment decisions. Further studies would be needed to increase the sample size and consider multicenter validation.

Abbreviations

ESCC
esophageal squamous cell carcinoma; CT:computed tomography; IBMs:imaging biomarkers; CCRT:concurrent chemoradiotherapy; AJCC, American Joint Committee on Cancer (AJCC) staging system (version 6.0); SCC, squamous cell carcinoma; PF, cisplatin and 5-fluorouracil; IMRT, intensity modulated radiation therapy; SMART, simultaneous modulated accelerated radiotherapy; GLCM, gray level co-occurrence matrices; GLRLM, gray level run-length matrices; NGTDM, neighborhood gray-tone difference matrices; GLSZM, gray level size-zone matrices; LASSO, least absolute shrinkage and selection operator; VIF, variance inflation factor; YI, Youden Index; DCA, decision curve analysis; ROC, receiver operation characteristic; AUC, area under the curve; CI, confidence interval; OS, overall survival; PFS, progression-free survival.

Declarations

Acknowledgments

Not applicable.

Funding

This study was supported by the following grants: Science and Technology Planning Project of Guangdong Province (2016ZC0166 and 2017ZC0279); Shantou University Medical College Clinical Research Enhancement Initiative (grant number: N0201424); Collaborative and Creative Center, Molecular Diagnosis and Personalized Medicine, Shantou University, Guangdong, China (grant number: 2501220302); Special Fund for Guangdong Science and Technology Innovation Strategy (grant number: 180918114960704); Project category of Medical and Health, Shantou, Guangdong Province,China (grant number: 190816095262212) ; Science and Technology Special Fund of Guangdong Province, China (190829105556145); Strategic and Special Fund for Science and Technology Innovatoin of Guangdong Province of China (180918114960704).Ethical Statement: The Shanghai Pulmonary Hospital institutional ethics committee approved this retrospective study.

Availability of data and materials

All data supporting the conclusions of this article is available upon request from the corresponding author.

Authors' contributions

Conception and design of the study: CBZ and CZC. Acquisition of data: CBZ and TTZ. Analysis and interpretation of the data: CBZ, TTZ and CZC. All authors participated in clinical data acquisition. Writing and revision of the manuscript: CBZ, TTZ, JZC and CZC. All authors read and approved the final manuscript.

Ethics approval and consent to participate

The Cancer Hospital of Shantou University Medical College institutional ethics committee approved this retrospective study (IRB No. 2019036), and the need for informed consent has been waived. This study complies with the standards of the Declaration of Helsinki and current ethics guidelines.

Consent for publication

Not applicable.

Competing interests

The authors have no conflicts of interest to declare.

Publisher's Note

Springer Nature remains neutral with regard to jurisdictional claims in published maps and institutional affiliations.

Author details

¹Cancer Hospital of Shantou University Medical College, Department of Radiation Oncology, Shantou City, China.

²CRUK/MRC Oxford Institute for Radiation Oncology, Department of Oncology- University of Oxford, Oxford, United Kingdom.

³Zhongshan City people's Hospital, Department of Radiation Oncology, Zhongshan City, China.

References

1. Bray F, Ferlay J, Soerjomataram I, et al. Global cancer statistics 2018: GLOBOCAN estimates of incidence and mortality worldwide for 36 cancers in 185 countries. *Cancer J Clin.* 2018;68:394–424. DOI:10.3322/caac.21492.

2. Kato K, Muro K, Minashi K, et al. Phase II study of chemoradiotherapy with 5-fluorouracil and cisplatin for Stage II-III esophageal squamous cell carcinoma: JCOG trial (JCOG 9906). *Int J Radiat Oncol Biol Phys*. 2011;81:684–90. DOI:10.1016/j.ijrobp.2010.06.033.
3. Minsky BD, Pajak TF, Ginsberg RJ, et al. INT 0123 (Radiation Therapy Oncology Group 94 – 05) phase III trial of combined-modality therapy for esophageal cancer: high-dose versus standard-dose radiation therapy. *Journal of clinical oncology: official journal of the American Society of Clinical Oncology*. 2002;20:1167–74. DOI:10.1200/jco.2002.20.5.1167.
4. Ohtsu A, Boku N, Muro K, et al. Definitive chemoradiotherapy for T4 and/or M1 lymph node squamous cell carcinoma of the esophagus. *Journal of clinical oncology: official journal of the American Society of Clinical Oncology*. 1999;17:2915–21. DOI:10.1200/jco.1999.17.9.2915.
5. Cooper JS, Guo MD, Herskovic A, et al. Chemoradiotherapy of locally advanced esophageal cancer: long-term follow-up of a prospective randomized trial (RTOG 85 – 01). *Radiation Therapy Oncology Group Jama*. 1999;281:1623–7. DOI:10.1001/jama.281.17.1623.
6. Gertler R, Stein HJ, Langer R, et al. Long-term outcome of 2920 patients with cancers of the esophagus and esophagogastric junction: evaluation of the New Union Internationale Contre le Cancer/American Joint Cancer Committee staging system. *Annals of surgery*. 2011;253:689–98. DOI:10.1097/SLA.0b013e31821111b5.
7. Hamai Y, Hihara J, Emi M, et al. Effects of Neoadjuvant Chemoradiotherapy on Pathological TNM Stage and Their Prognostic Significance for Surgically-treated Esophageal Squamous Cell Carcinoma. *Anticancer research*. 2017;37:5639–46. DOI:10.21873/anticancer.11999.
8. Oweira H, Schmidt J, Mehrabi A, et al. Validation of the eighth clinical American Joint Committee on Cancer stage grouping for esophageal cancer. *Future oncology (London England)*. 2018;14:65–75. DOI:10.2217/fon-2017-0376.
9. Chen CZ, Chen JZ, Li DR, et al. Long-term outcomes and prognostic factors for patients with esophageal cancer following radiotherapy. *World J Gastroenterol*. 2013;19:1639–44. DOI:10.3748/wjg.v19.i10.1639.
10. Chen M, Huang J, Zhu Z, et al. Systematic review and meta-analysis of tumor biomarkers in predicting prognosis in esophageal cancer. *BMC Cancer*. 2013;13:539. DOI:10.1186/1471-2407-13-539.
11. Qiao Y, Chen C, Yue J, et al. Tumor marker index based on preoperative SCC and CYFRA 21 – 1 is a significant prognostic factor for patients with resectable esophageal squamous cell carcinoma. *Cancer Biomark A*. 2019;25:243–50. DOI:10.3233/cbm-190058.
12. Lambin P, Rios-Velazquez E, Leijenaar R, et al. Radiomics: extracting more information from medical images using advanced feature analysis. *European journal of cancer (Oxford England: 1990)*. 2012;48:441–6. DOI:10.1016/j.ejca.2011.11.036.
13. Aerts HJ, Velazquez ER, Leijenaar RT, et al. Decoding tumour phenotype by noninvasive imaging using a quantitative radiomics approach. *Nature communications*. 2014;5:4006. DOI:10.1038/ncomms5006.

14. Gillies RJ, Kinahan PE, Hricak H, Radiomics. Images Are More than Pictures. They Are Data *Radiology*. 2016;278:563–77. DOI:10.1148/radiol.2015151169.
15. Ganeshan B, Skogen K, Pressney I, et al. Tumour heterogeneity in oesophageal cancer assessed by CT texture analysis: preliminary evidence of an association with tumour metabolism, stage, and survival. *Clinical radiology*. 2012;67:157–64. DOI:10.1016/j.crad.2011.08.012.
16. Yip C, Landau D, Kozarski R, et al. Primary esophageal cancer: heterogeneity as potential prognostic biomarker in patients treated with definitive chemotherapy and radiation therapy. *Radiology*. 2014;270:141–8. DOI:10.1148/radiol.13122869.
17. Hou Z, Ren W, Li S, et al. Radiomic analysis in contrast-enhanced CT: predict treatment response to chemoradiotherapy in esophageal carcinoma. *Oncotarget*. 2017;8:104444–54. DOI:10.18632/oncotarget.22304.
18. Larue R, Klaassen R, Jochems A, et al. Pre-treatment CT radiomics to predict 3-year overall survival following chemoradiotherapy of esophageal cancer. *Acta oncologica (Stockholm Sweden)*. 2018;57:1475–81. DOI:10.1080/0284186x.2018.1486039.
19. Cheng L, Wu L, Chen S, et al [CT-based radiomics analysis for evaluating the differentiation degree of esophageal squamous carcinoma]. *Zhong nan da xue xue bao Yi xue ban = Journal of Central South University Medical sciences* 2019; 44: 251–256. DOI: 10.11817/j.issn.1672-7347.2019.03.004.
20. Xie C, Yang P, Zhang X, et al. Sub-region based radiomics analysis for survival prediction in oesophageal tumours treated by definitive concurrent chemoradiotherapy. *EBioMedicine*. 2019;44:289–97. DOI:10.1016/j.ebiom.2019.05.023.
21. Ge X, Yang X, Lu X, et al. Long-term clinical outcome of intensity-modulated radiation therapy for locally advanced esophageal squamous cell carcinoma. *Tumori*. 2015;101:168–73. DOI:10.5301/tj.5000234.
22. Chen J, Guo H, Zhai T, et al. Radiation dose escalation by simultaneous modulated accelerated radiotherapy combined with chemotherapy for esophageal cancer: a phase II study. *Oncotarget*. 2016;7:22711–9. DOI:10.18632/oncotarget.8050.
23. Haralick RM, Shanmugam K, Dinstein I, Textural Features for Image Classification. *IEEE Transactions on Systems Man Cybernetics*. 1973;SMC-3:610–21. DOI:10.1109/TSMC.1973.4309314.
24. Galloway M. Texture analysis using gray level run lengths. *Comput Graph Image Proc*. 1974;4:172–99.
25. Sun C, Wee WG. Neighboring gray level dependence matrix for texture classification. *Computer Vision, Graphics, and Image Processing* 1983; 23: 341–352. DOI: [https://doi.org/10.1016/0734-189X\(83\)90032-4](https://doi.org/10.1016/0734-189X(83)90032-4).
26. Thibault G, Fertil B, Navarro C, et al Texture Indexes and Gray Level Size Zone Matrix Application to Cell Nuclei Classification, 2009.
27. Lambin P, Leijenaar RTH, Deist TM, et al. Radiomics: the bridge between medical imaging and personalized medicine. *Nature reviews Clinical oncology*. 2017;14:749–62. DOI:10.1038/nrclinonc.2017.141.

28. Hall M Correlation-based Feature Selection for Discrete and Numeric Class Machine Learning, 2000; 359–366.
29. Friedman J, Hastie T, Tibshirani R. Regularization Paths for Generalized Linear Models via Coordinate Descent. *Journal of statistical software*. 2010;33:1–22.
30. Zhai TT, van Dijk LV, Huang BT, et al. Improving the prediction of overall survival for head and neck cancer patients using image biomarkers in combination with clinical parameters. *Radiotherapy oncology: journal of the European Society for Therapeutic Radiology Oncology*. 2017;124:256–62. DOI:10.1016/j.radonc.2017.07.013.
31. Chen LL, Nolan ME, Silverstein MJ, et al. The impact of primary tumor size, lymph node status, and other prognostic factors on the risk of cancer death. *Cancer*. 2009;115:5071–83. DOI:10.1002/cncr.24565.
32. van Griethuysen JJM, Fedorov A, Parmar C, et al. Computational Radiomics System to Decode the Radiographic Phenotype. *Cancer research*. 2017;77:e104–7. DOI:10.1158/0008-5472.Can-17-0339.
33. Lee G, Lee HY, Park H, et al. Radiomics and its emerging role in lung cancer research, imaging biomarkers and clinical management: State of the art. *Eur J Radiol*. 2017;86:297–307. DOI:10.1016/j.ejrad.2016.09.005.
34. Tixier F, Le Rest CC, Hatt M, et al. Intratumor heterogeneity characterized by textural features on baseline 18F-FDG PET images predicts response to concomitant radiochemotherapy in esophageal cancer. *Journal of nuclear medicine: official publication Society of Nuclear Medicine*. 2011;52:369–78. DOI:10.2967/jnumed.110.082404.
35. Mule S, Thieffn G, Costentin C, et al. Advanced Hepatocellular Carcinoma: Pretreatment Contrast-enhanced CT Texture Parameters as Predictive Biomarkers of Survival in Patients Treated with Sorafenib. *Radiology*. 2018;288:445–55. DOI:10.1148/radiol.2018171320.
36. Janmaat VT, Steyerberg EW, van der Gaast A, et al Palliative chemotherapy and targeted therapies for esophageal and gastroesophageal junction cancer. *The Cochrane database of systematic reviews* 2017; 11: Cd004063. DOI: 10.1002/14651858.CD004063.pub4.
37. Bolm L, Kasmann L, Paysen A, et al. Multimodal Anti-tumor Approaches Combined with Immunotherapy to Overcome Tumor Resistance in Esophageal and Gastric Cancer. *Anticancer research*. 2018;38:3231–42. DOI:10.21873/anticancer.12588.
38. Hayes T, Smyth E, Riddell A, et al. Staging in Esophageal and Gastric Cancers. *Hematol Oncol Clin N Am*. 2017;31:427–40. DOI:10.1016/j.hoc.2017.02.002.
39. Win T, Miles KA, Janes SM, et al. Tumor heterogeneity and permeability as measured on the CT component of PET/CT predict survival in patients with non-small cell lung cancer. *Clinical cancer research: an official journal of the American Association for Cancer Research*. 2013;19:3591–9. DOI:10.1158/1078-0432.Ccr-12-1307.
40. Badic B, Desseroit MC, Hatt M, et al. Potential Complementary Value of Noncontrast and Contrast Enhanced CT Radiomics in Colorectal Cancers. *Acad Radiol*. 2019;26:469–79. DOI:10.1016/j.acra.2018.06.004.

41. Moons KG, Altman DG, Reitsma JB, et al. Transparent Reporting of a multivariable prediction model for Individual Prognosis or Diagnosis (TRIPOD): explanation and elaboration. *Ann Intern Med.* 2015;162:W1–73. DOI:10.7326/m14-0698.

Figures

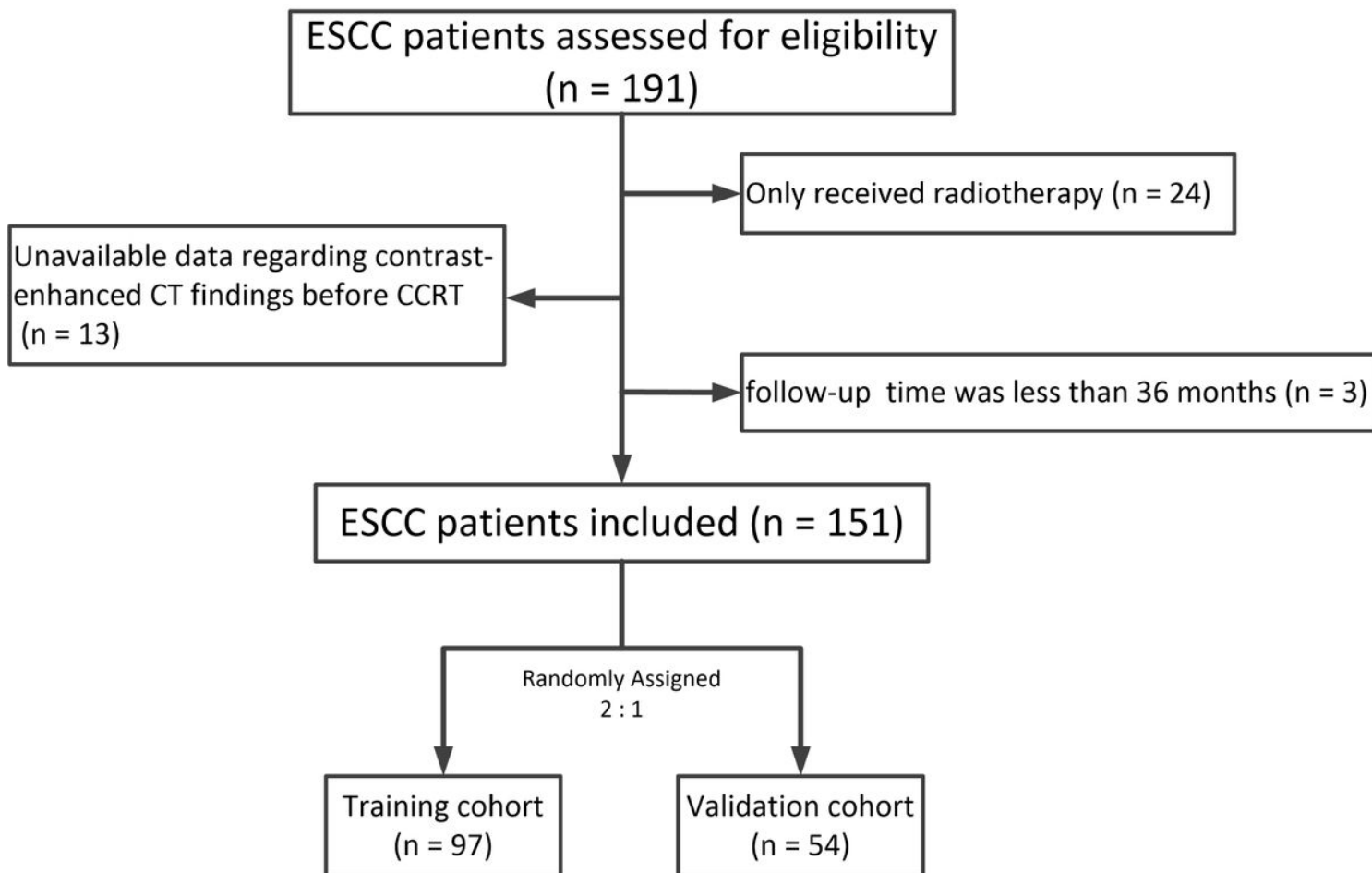
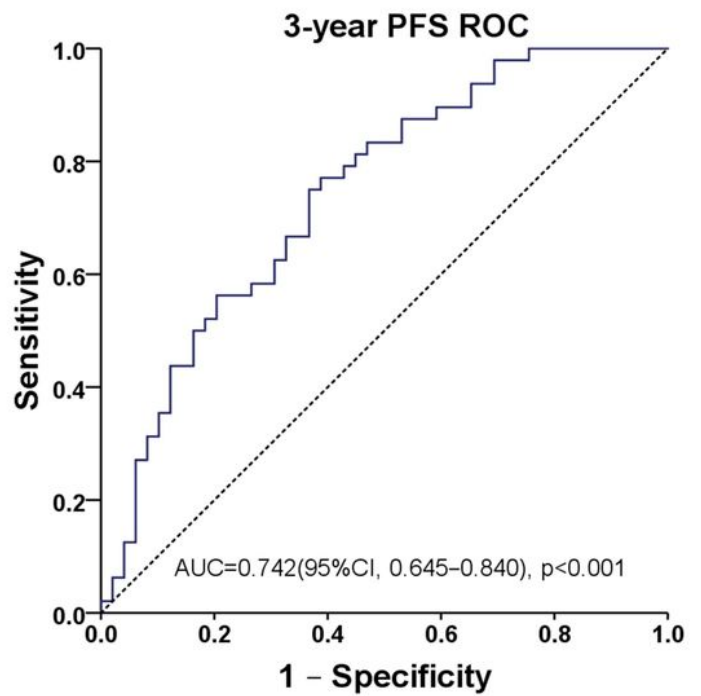
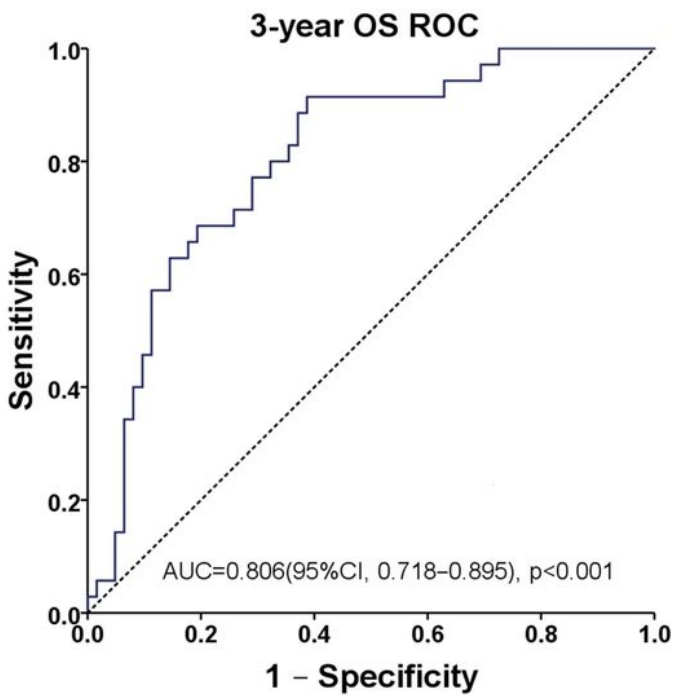


Figure 1

Flowchart of study inclusion in the present study. Abbreviations: ESCC, esophageal squamous cell carcinoma; CCRT, concurrent chemoradiotherapy; CT, computed tomography.

A Training cohort



B Validation cohort

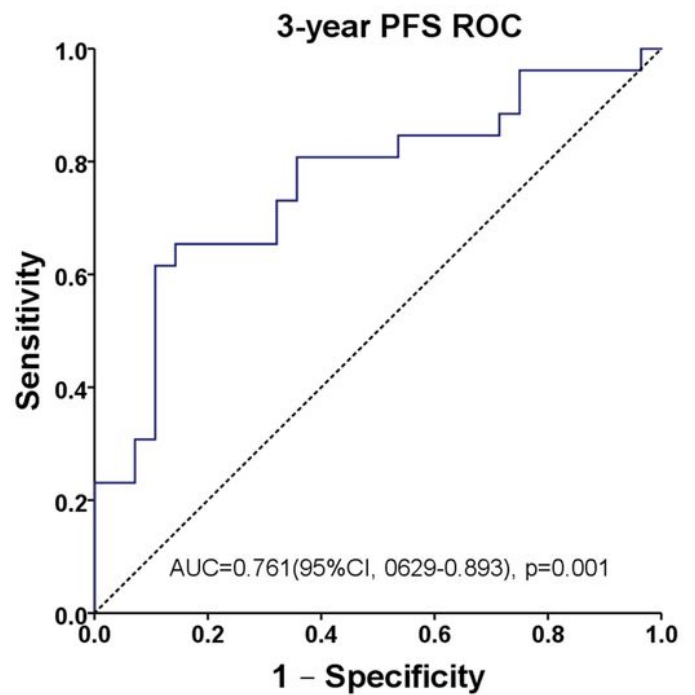
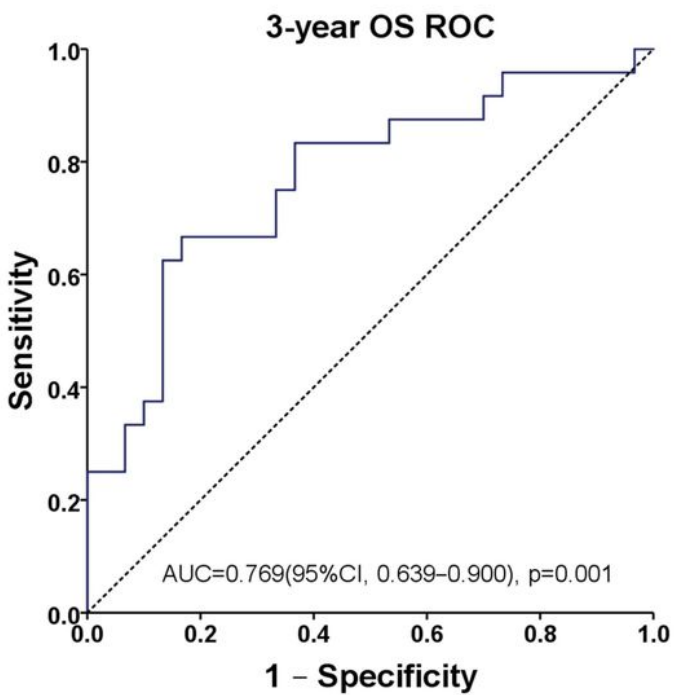
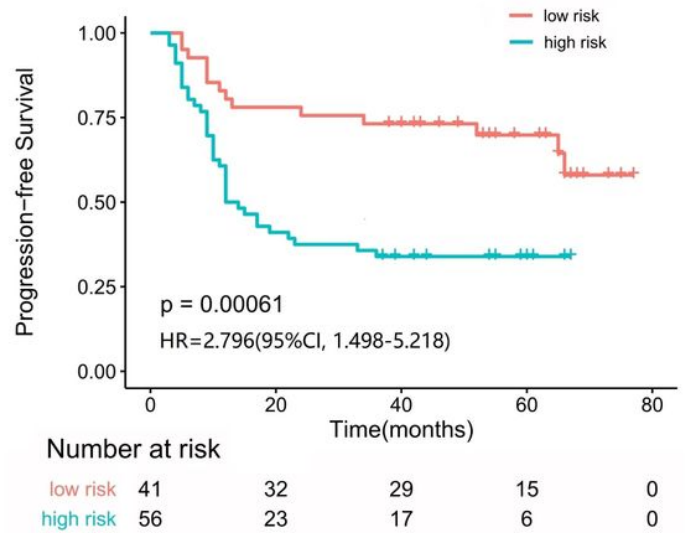
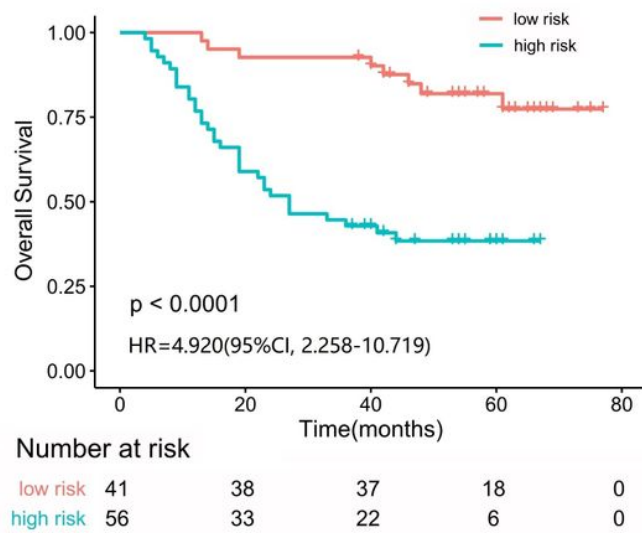


Figure 2

IBM score measured by 3-year ROC curves in the (A) Training cohort and (B) Validation cohort. We used AUCs to assess prognostic accuracy for two cohorts, respectively. Abbreviations: ROC, receiver operation characteristic; AUC, area under the curve; CI, confidence interval; OS, overall survival; PFS, progression-free survival; IBM, image biomarker.

A Training cohort



B Validation cohort

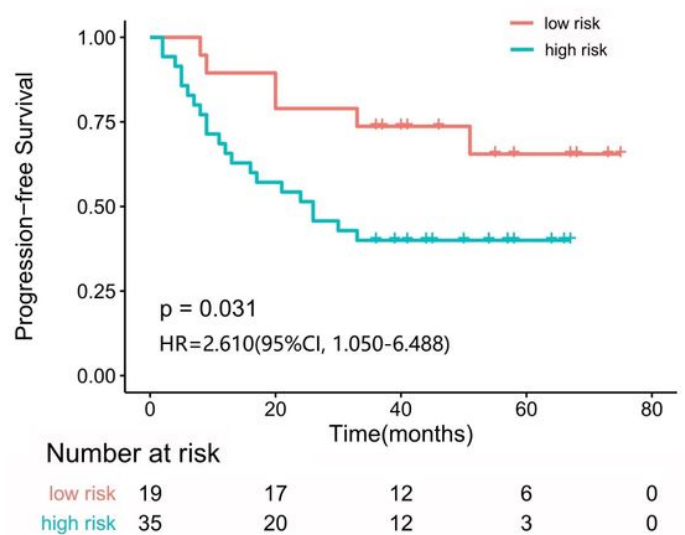
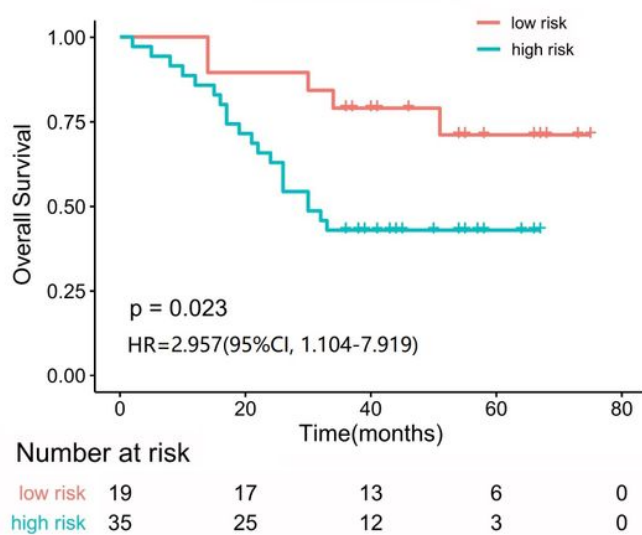
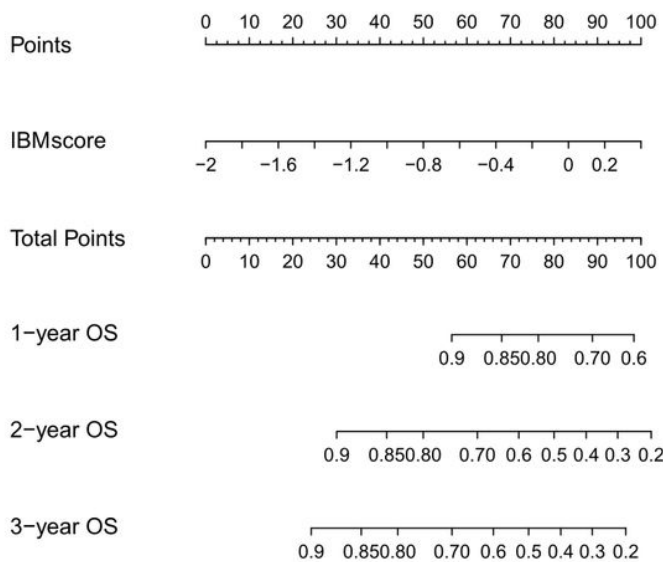
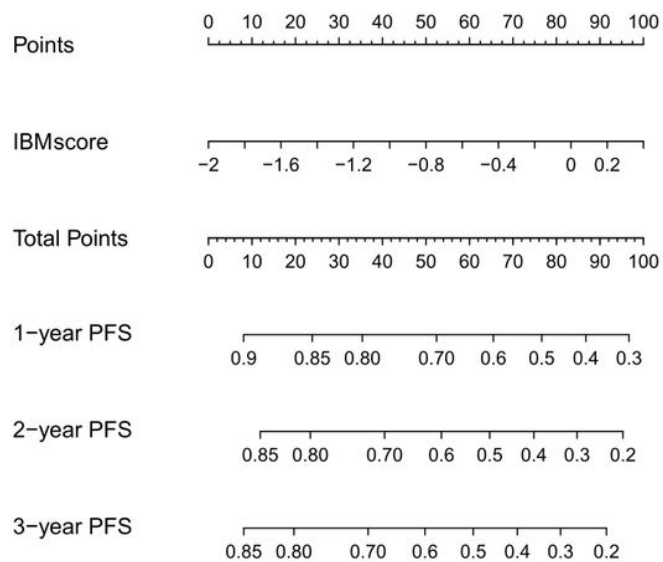


Figure 3

Kaplan–Meier survival analysis of overall survival and progression-free survival according to the optimum cutoffs of IBM score. Patients stratified by risk subgroups for (A) Training cohort and (B) Validation cohorts. We calculated p-value using the log-rank test. Abbreviations: HR, hazard ratio; IBM, image biomarker.



IBM nomogram for OS

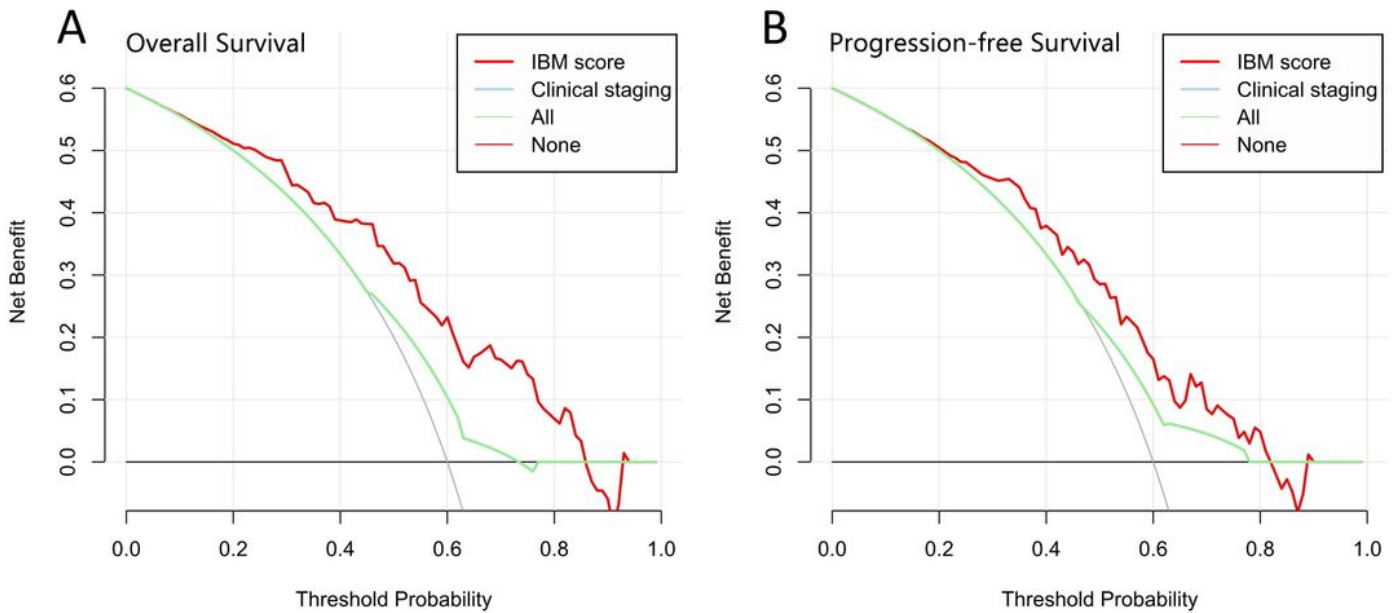


IBM nomogram for PFS

Figure 4

IBMs nomograms for OS (left) and PFS (right). The constructed IBMsnomograms were used to estimate OS and PFS for ESCC.

Training Cohort



Validation Cohort

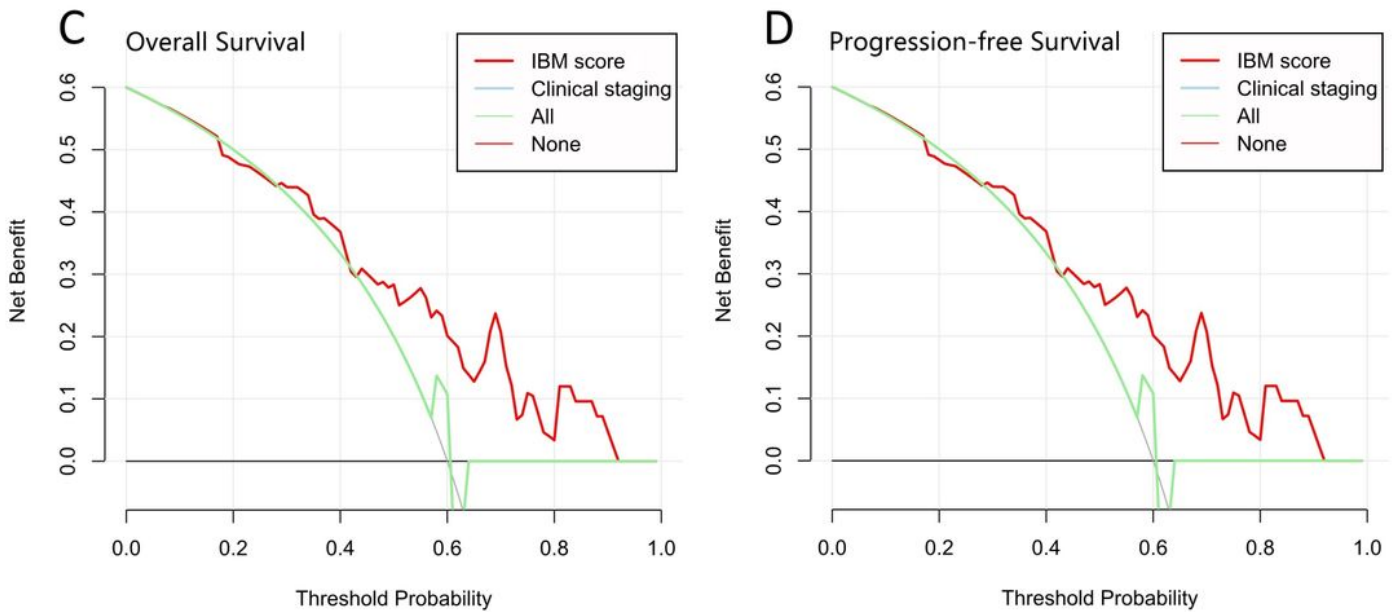


Figure 5

Decision curve analysis for the IBM score and clinical stage nomogram in the training and validation cohort. The y-axis represented the net benefit. The x-axis represented the threshold probability. Across the full range of threshold probabilities, the horizontal black line indicated that no patient chose to undergo follow-up, and the oblique grey line indicated that all patients underwent follow-up. The red line

represented IBM score. The light green line represented clinical stage. Compared to the clinical stage, the IBM score had the higher net benefit.

Supplementary Files

This is a list of supplementary files associated with this preprint. Click to download.

- [SupplementaryMaterials.pdf](#)